Modelling, Simulation and Control of Pedestrian Avoidance Maneuver for an Urban Electric Vehicle

L. Alonso Rentería and J. M. Pérez Oria
Department of Electronics Technology, Systems Engineering and Automatics
University of Cantabria
Santander, Spain
e-mail: [luciano.alonso, juan.perezoria]@unican.es

A. Jiménez Avello and Basil Mohammed Al-Hadithi
Intelligent Control Group
Polytechnic University of Madrid, Automation and Robotics Center (UPM-CISC)
Madrid, Spain
e-mail: [agustin.jimenez, basil.alhadithi]@upm.es

V. M. Becerra
School of Systems Engineering
University of Reading
Reading, United Kingdom
e-mail: v.m.becerra@reading.ac.uk

***Abstract*— The mathematical model of an electric vehicle, as well as the control system for avoiding pedestrians in urban traffic is described. The vehicle is modeled as a continuous system consisting of several subsystems. In addition, a set of sensors and actuators along with a two-level discrete control system are modeled. Based on this model, a pedestrian avoidance maneuver for typical speeds in city traffic is simulated. When the sensory system detects a pedestrian in the vehicle's path, the decision system calculates its trajectory. Using this information, the speed and/or direction that the vehicle must take in order to avoid the accident are estimated. These values are sent to the low-level controllers of the accelerator/brake and steering, which generate the signals to be applied to such systems to achieve the desired trajectory and speed.**

Keywords- modeling; simulation; electric vehicle; urban traffic; pedestrian avoidance

I. INTRODUCTION

According to the Statistical Yearbook of Accidents 2013 [1], about 58% of road accidents with casualties occurred in urban traffic. Almost 17% of the victims were pedestrians. The human factor (alcohol, fatigue, distractions) is the main cause of these accidents, ahead of external factors such as road or weather conditions. For some years, vehicle manufacturers incorporate many widely known active safety systems, such as Antilock Brake System, Electronic Stability Control System, or Traction Control System. All these systems are highly efficient to avoid losing the control of the vehicle in difficult circumstances, thus protecting the passengers inside, but not to the pedestrians nor other vehicles. In recent times, manufacturers and other institutions are investigating seriously in innovative safety systems that warn the driver in case of danger of a frontal collision, or even able to activate the brakes if necessary. Most of them are based on a combination of radar and cameras [2]. Recently, Toyota announced its "Pedestrian-Avoidance Steer Assist System", capable of acting on the steering wheel when the braking is not enough to avoid the accident [3].

In recent years, there have been many contributions in this subject. For example, in [4] a stereo vision system is used to measure the position and relative speed of the pedestrian. When a collision is considered unavoidable, the pedestrian protection systems are activated, such as active braking system. Otherwise, a fuzzy system takes control of the steering wheel and makes a lane change maneuver, regardless of the presence of other objects. In [5], the uncertainty of the intention of the pedestrian is incorporated into the process. Then, solving a Mixed Observable Markov Decision Process (MOMDP), a robust pedestrian avoidance policy is generated, but the speed is limited to 2 m/s.

In this work, the mathematical model of an electric urban vehicle along with a set of sensors and actuators, which can be seen in Fig. 1, is presented. This model has allowed the development and simulation of a control system for a pedestrian avoidance maneuver, capable of acting on the brakes, as well as on the steering if necessary. Since not all the sensors and actuators have been already installed in the experimental vehicle, the maneuver has not been verified experimentally. The team expects to complete this task in a short time, along with the fine tuning of the model. The present work is a further contribution of the research group in the field of active safety and intelligent vehicles, to be added to those made in recent years [6][7][8][9].

The rest of the paper is organized as follows: the mathematical model of the vehicle, along with sensors and actuators involved in the maneuver is described in section II; section III explains the control algorithm; in section IV the results of simulations are shown and analyzed; finally, a section with the main conclusions is included.

Figure 1. Experimental electric vehicle

II. MATHEMATICAL MODEL OF THE VEHICLE

Based on [10][11][12], a mathematical model of the experimental electric vehicle has been developed. Some model parameters have been directly measured, others have been analytically estimated, and others have been manually tuned with reasonable values, so that the behavior of the model approximates the actual experimental vehicle. Fig. 2 shows the main dimensions of the vehicle.

Three reference frames are considered: an inertial system fixed on the road, to describe the absolute position and orientation of the vehicle; a system located at the center of gravity, whose *x* axis coincides with the longitudinal axis, to describe the forces and torques acting on the body of the car; finally, a reference frame on each wheel, to describe the forces and torques exerted on it. This can be seen in Fig. 3. Due to space limitations, it is assumed that readers are familiar with the equations of coordinate transformation between different reference systems. In addition, all units are in the International System, thus omitted.

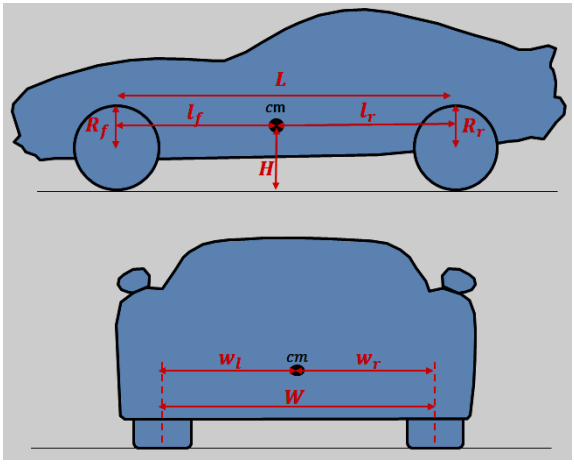

Figure 2. Geometric parameters involved in vehicle dynamics.

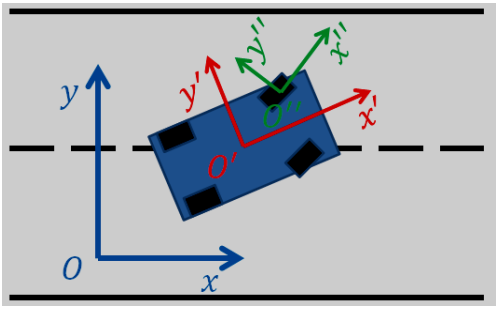

Figure 3. Reference frames.

The system has three degrees of freedom: the *x* and *y* coordinates of the center of gravity and the heading angle Φ (angle between x' and x axes), expressed in the inertial system. In what follows, each submodel is described.

A. Tires

Fig. 4 shows the geometry of the mathematical model of the tires. $\overrightarrow{\omega R}$ is the linear velocity vector due to pure rotation; $\vec{v}$ is the effective velocity vector of the tire; α is the angle between both vectors; the vector $\vec{s} = \overrightarrow{\omega R} - \vec{v}$ is called *slip vector*, responsible for the forces between the tire and the road, being s_l and s_t its components in the coordinate system of the wheel; δ is the orientation of the tire relative to the longitudinal axis of the vehicle, being determined by the steering wheel position for the front wheels, and being zero for the rear ones; $\vec{F}$ is the force acting on the tire due to the slip vector, being f_l and f_t its longitudinal and transverse components in the coordinate system of the tire. This force is given by the expression:

$$\vec{F} = \vec{\mu} F_z \qquad (1)$$

being F_z the vertical load on the tire, and $\vec{\mu} = (\mu_l, \mu_t)$ a vector whose components are the friction coefficients in the longitudinal and transverse directions. In order to obtain these friction coefficients, it is necessary to normalize the slip vector:

$$\vec{s}' = \frac{\vec{s}}{\max(|\overrightarrow{\omega R}|, |\vec{v}|)} \qquad (2)$$

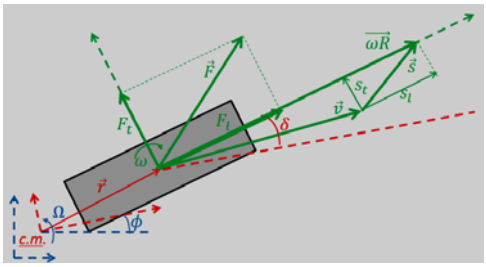

Figure 4. Geometric model of the tires.

then, the *magic formula* of Pacejka is applied:

$$\psi = B\, s'_{l,t}$$
$$\mu_{l,t} = D\sin(C\arctan(\psi - E(\psi - \arctan(\psi)))) \quad (3)$$

Parameters B, C, D and E were experimentally obtained by Hans B. Pacejka for different surfaces (in this paper dry asphalt is assumed).

B. Wheels

In Fig. 5 the forces and torques involved in the dynamics of a wheel are shown, which responds to the equation:

$$J\,\dot{\omega} = T_w - T_b + R(F_r - F_l) \quad (4)$$

where J is the inertia of the wheel; T_w is the traction torque provided by the engine through the transmission, being zero for the rear wheels; T_b is the braking torque exerted by the brake caliper; F_r is the rolling resistance; lastly F_l is the longitudinal force on the tire seen in subsection *A*. F_r is proportional to the rotational speed of the wheel:

$$F_r = C_f\,\omega \quad (5)$$

C_f depending on the types of asphalt and tire.

C. Transmission and differential

The transmission and the differential are modeled as a single gain G. As it can be seen in Fig. 6, through this gain the torque T_e provided by the engine is transmitted equally to both front wheels, and the mean of their rotational speeds, ω_{fl} and ω_{fr}, is converted in motor speed ω_e:

$$T_w = G\,T_e/2$$
$$\omega_e = G(\omega_{fl} + \omega_{fr})/2 \quad (6)$$

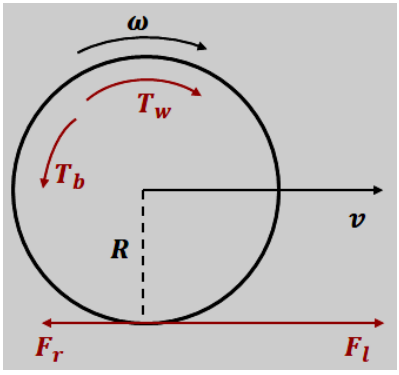

Figure 5. Wheel dynamics.

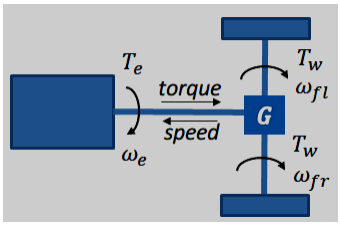

Figure 6. Transmission model.

D. Electric motor

The propulsion system is a DC motor, whose model can be seen in Fig. 7, and whose equations are, as it is well known:

$$\frac{di}{dt} = \frac{v - R\,i - e}{L}$$
$$T_e = T - J\frac{d\omega_e}{dt} - B\,\omega_e \quad (7)$$
$$e = K_e\,\omega_e$$
$$T = K_t\,i$$

where R and L are the resistance and inductance of the winding, B and J are the friction coefficient and moment of inertia of the rotor, v and i are the armature voltage and the current through the winding, ω_e and e are the rotational speed and the counter-electromotive force (BEMF), K_t and K_e are the torque constant and the BEMF constant, and lastly, T and T_e are the electromagnetic torque and the mechanical torque delivered to the transmission.

Both ω_e and $\dot{\omega}_e$ are taken as the average values of the speed and accelerations of the front wheels, multiplied by the gain of the transmission and the differential.

The voltage v applied to the motor is a fraction of the maximum voltage v_{max} given by the position of the accelerator pedal.

E. Brakes

The hydraulic brake circuit is modeled as a first order system:

$$P_b(s) = \frac{K_c}{1 + \tau_b s}U_b(s) \quad (8)$$

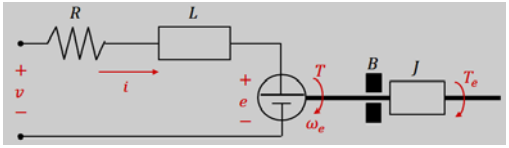

Figure 7. Electric motor.

where p_b is the pressure, u_b is the position of the brake pedal, τ_b is the time constant and K_c is the steady state gain. The braking torque is considered proportional to this pressure and to the rotational speed for small values of the latter, according to the following expression:

$$T_b = K_b\, p_b \min(1, \frac{\omega}{0.1}) \qquad (9)$$

where K_b is the constant of proportionality, which is in general different for the front and rear wheels.

F. Steering system

Fig. 8 shows the geometry of an Ackermann steering system. The input is the angular position of the steering wheel δ_v. The steering column is modeled as a reduction K_δ, so that the output is the angle δ of a hypothetical wheel in the center of the front axle, with respect to the longitudinal axis of the vehicle. With this system, the front wheels are in general oriented differently, since in the curves they follow different paths. These angles are given by:

$$\delta = K_\delta\, \delta_v$$

$$\delta_l = \arctan\left(\frac{L\tan(\delta)}{L - 0.5W\tan(\delta)}\right) \qquad (10)$$

$$\delta_r = \arctan\left(\frac{L\tan(\delta)}{L + 0.5W\tan(\delta)}\right)$$

where W is the length of the front axle, and L is the distance between the front and rear axles.

G. Vehicle body

Fig. 9 shows the forces acting on the body of the vehicle. For each longitudinal force subscripted with "x", there is a corresponding lateral force subscripted with "y", although it is not shown in the figure for clarity. In the same way, only the wheels on the left side of the vehicle are shown.

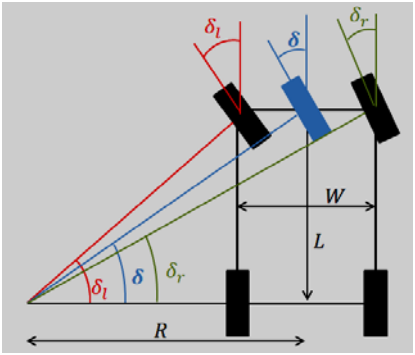

Figure 8. Ackermann steering system.

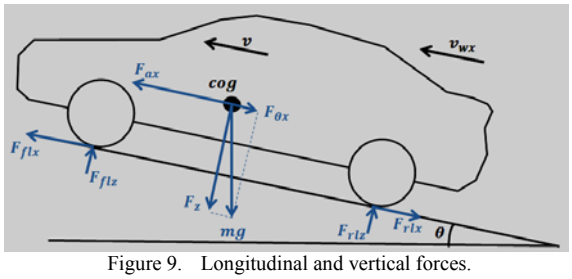

Figure 9. Longitudinal and vertical forces.

The linear acceleration of the center of gravity is given by:

$$m\ddot{\vec{r}} = \vec{F}_{fl} + \vec{F}_{fr} + \vec{F}_{rl} + \vec{F}_{rr} + \vec{F}_\theta + \vec{F}_a \qquad (11)$$

where:

- m: mass of the vehicle
- $\ddot{\vec{r}}$: acceleration of the center of gravity
- $\vec{F}_{ij}(i = f, r \quad j = l, r)$: horizontal tire forces
- $\vec{F}_\theta$: force due to the slope of the road:

$$\vec{F}_\theta = -m\,g\sin(\theta)\left(\cos(\phi), \sin(\phi)\right) \qquad (12)$$

- $\vec{F}_a$: aerodynamic drag. Making $\varphi = x, y$ then:

$$F_{a\varphi} = 0.5\,\rho\, C_d\, A_\varphi \left(v_{w\varphi} - \dot{\varphi}\right)^2 sign\left(v_{w\varphi} - \dot{\varphi}\right) \qquad (13)$$

where ρ is the air density, C_d is the drag coefficient, $\vec{v}_w$ is the wind velocity, and A_φ and $\dot{\varphi}$ are the projected area and the speed of the vehicle along the corresponding axis.

Both the wind velocity and the slope of the road are taken as zero in this paper.

The angular acceleration around the z axis is expressed by:

$$J\ddot{\phi} = T_{fl} + T_{fr} + T_{rl} + T_{rr} \qquad (14)$$

where J is the moment of inertia of the car around its vertical axis, Φ is the angle between the longitudinal axis of the car and the x axis of the inertial reference system, and T_{ij} is the torque due to force F_{ij}.

There is a weight transfer towards the rear axle when car is accelerating, and towards the front axle during braking. In the same way, some weight is transferred towards the left wheels when turning to the right, and towards the right wheels when turning to the left. That is, the vertical load on each tire changes depending on the longitudinal and transverse accelerations. The loads on the front and rear axles are calculated according to:

$$F_{zf} = \frac{m}{L}\left(g\cos(\theta)l_r - H\ddot{x}\right)$$
$$F_{zr} = \frac{m}{L}\left(g\cos(\theta)l_f + H\ddot{x}\right) \quad (15)$$

From these, the vertical load on each tire can be obtained:

$$F_{zfl} = \frac{1}{W}\left(F_{zf}w_r - mH\ddot{y}\right)$$
$$F_{zfr} = \frac{1}{W}\left(F_{zf}w_l + mH\ddot{y}\right)$$
$$F_{zrl} = \frac{1}{W}\left(F_{zr}w_r - mH\ddot{y}\right) \quad (16)$$
$$F_{zrr} = \frac{1}{W}\left(F_{zr}w_l + mH\ddot{y}\right)$$

H. Integration algorithm

In order to integrate the described ordinary differential equations, a numerical method is necessary. Each second-order differential equation is transformed into a system of two first-order differential equations. Then the well-known Runge-Kutta-Fehlberg RKF45 method [13] is used to solve the overall system. It embeds two explicit Runge-Kutta methods with orders 4 and 5 to estimate the local truncation error and adapt the time step size.

III. CONTROL SYSTEM

The control algorithm runs with a sampling time $T_s = 0.1$ seconds. Firstly a sample is taken from each one of the sensors involved in the maneuver. With this information, the position and velocity of the pedestrian relative to the vehicle are calculated. Then, the speed and direction necessary to prevent the accident are estimated and supplied to the low level controllers, which send the necessary control signals to the actuators.

A. Sensors

Several sensors are modeled trying to emulate the operation of which will be installed in the actual experimental vehicle:

- A stereo vision system that detects and locates the relative position $\vec{r}_k = (x_k, y_k)$ of the pedestrians in the path of the vehicle, placed beside the rear view mirror. It is modeled as a function taking as inputs the absolute position and orientation of the car, and the absolute position of the pedestrian. If he is within the visual field of the camera, then his vector of relative position is returned, otherwise the returned value is the zero vector.
- A nine degrees of freedom inertial unit, located as close as possible to the center of gravity of the vehicle, and aligned with its main axes. It provides three linear accelerations, three rotational speeds, and three components of the Earth's magnetic field. This sensor is modeled as a function that takes as input the state vector of the car, and returns the nine appropriate values.
- A Hall effect sensor placed on the motor shaft, to estimate the longitudinal speed of the vehicle. It is modeled with a function returning the rotational speed of the motor. This speed is divided by the gain of the transmission and the differential, and multiplied by the radius of the wheels, to return the car speed.

B. Low level controllers

To control the steering wheel a proportional (P) regulator is used. The accelerator and the brake are controlled by a single proportional-integral (PI) controller, whose output is applied on the accelerator when positive, and on the brake when negative. Their outputs are normalized between -1 and 1.

C. Control algorithm

Fig. 10 shows the geometric problem, with all dimensions in meters. The vehicle with the camera, the region of interest and a pedestrian in it are shown.

The operation of the control algorithm begins when a pedestrian is detected in two consecutive images within the region of interest. Then:

1. From two successive measurements of the relative position, the relative velocity of the pedestrian at time k is estimated:

$$\vec{v} = \frac{\vec{r}_k - \vec{r}_{k-1}}{T_s} = (v_x, v_y) \quad (17)$$

2. If $v_x > 0$, that is, if the pedestrian moves away from the vehicle, the algorithm terminates without any control action. If $v_x \le 0$, the pedestrian is approaching the vehicle, and the *time to collision* t_c and the relative lateral position y_c at this time are predicted:

$$t_c = -\frac{x_k - 1}{v_x} \quad (18)$$

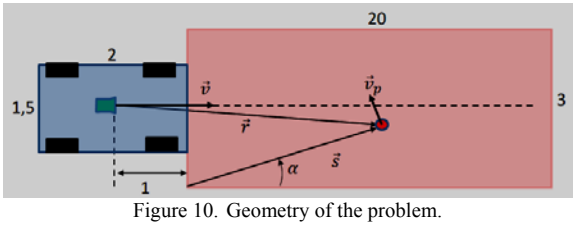

Figure 10. Geometry of the problem.

$$y_c = y_k + v_y t_c \quad (19)$$

3. If $|y_c| > 1.5$, that is, if the pedestrian leaves the region of interest before the time of collision, no accident will occur, and the algorithm terminates without any control action. Else, the longitudinal deceleration required to stop the vehicle at that time is computed:

$$a_x = v_x / t_c \quad (20)$$

The difference between this and the longitudinal acceleration measured by the inertial system is the input to the low level PI controller of the accelerator/brake, which provides the necessary signals to the electric motor and to the brake system. That is, the deceleration is controlled instead of the speed.

4. If $t_c > 1$ there is no need to steer, and the algorithm terminates without action on the steering wheel, else the vector $\vec{s}$ from the nearest corner of the vehicle to the current position of the pedestrian is calculated:

$$\vec{s} = \vec{r}_k - (1, 1.5\, sign(y_k)) \quad (21)$$

5. The angle α of this vector relative to the longitudinal axis of the vehicle is calculated:

$$\alpha = \arctan(s_y / s_x) \quad (22)$$

This angle is the input to the low level P controller of the steering wheel, trying to keep the pedestrian on the edge of the region of interest.

Fig. 11 sows the flow chart of this algorithm.

IV. Results

In this work, the presence of other obstacles in the vicinity has not been taken into account, for example a vehicle overtaking, or circulating in the opposite direction by the adjacent lane, or parked on the right side of the road. In these circumstances, an accident with more serious consequences could be caused, even transferring the legal responsibility to the driver, although the pedestrian was the real responsible. To make the presented maneuver completely safe, the sensory system should detect these situations and inform to the control system, which could then decide on the safest maneuver.

Fig. 12 shows the temporal representation of the main magnitudes observed in a typical scenario. In Fig. 13, a sequence of pictures is shown with the positions of the vehicle and the pedestrian at different times in the simulation. As shown in both, initially the vehicle travels at a constant speed of 40 km/h. At 33 seconds, a pedestrian is detected inside the region of interest, and the vehicle begins to decelerate, while maintaining its direction. Finally, at 36.8 seconds, the vehicle is completely stopped just in front of the pedestrian. As can be seen in Fig. 12 (d), there is no action on the steering wheel.

In another scenario (Figs. 14 and 15), the vehicle is traveling at an initial speed of 44 km / h. At the second 30.8 a pedestrian is detected within the region of interest, and the vehicle starts to brake. As the distance is too small to avoid the accident only by brake, an evasive action is done by modifying the vehicle's path. As it can be seen, at second 31.9 the vehicle overtakes the pedestrian at a speed of 21.2 km/h. Finally, at the second 32.9, the vehicle has completely surpassed the pedestrian, without reaching a complete stop.

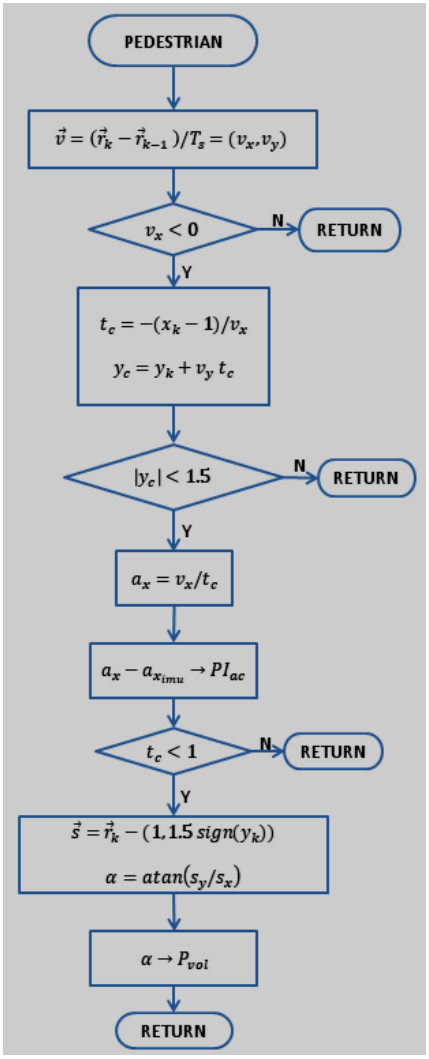

Figure 11. A flow chart showing the control algorithm.

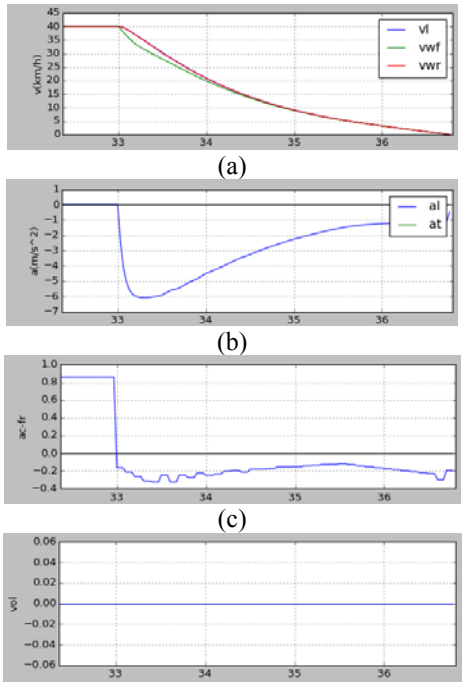

Figure 12. Temporal representation of the main variables in a simulation in which the vehicle is completely stopped, without steering action. a) Longitudinal speed of the car (blue), and mean of the rotational speeds of the front wheels (green) and rear wheels (red), in km/h. b) Longitudinal (blue) and lateral (green) accelerations, in m/s^{-2}. c) Control signal for the accelerator/brake, in percentage. d) Control signal for the steering wheel, in percentage.

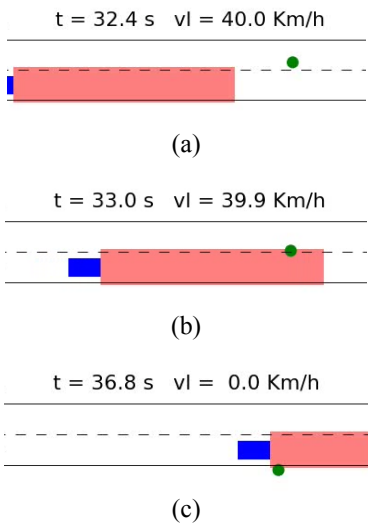

Figure 13. Sequence of images of a simulation in which the vehicle completely stops, without steering acction. At the top of each picture, the time and the longitudinal speed of the vehicle are observed.

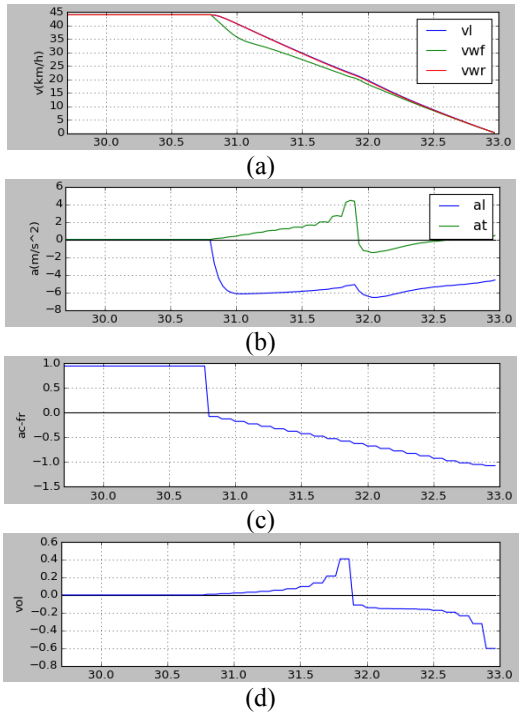

Figure 14. Temporal representation of the main variables in a simulation in which the vehicle steers to avoid the accident.

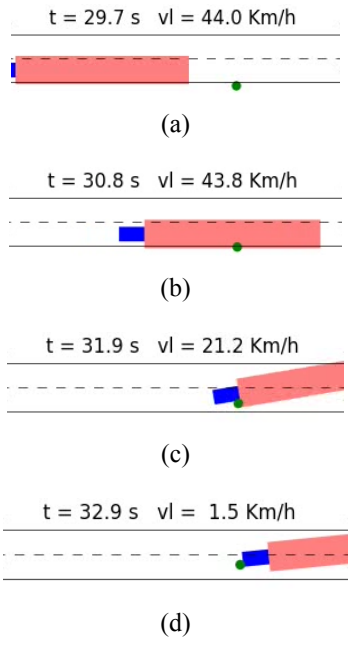

Figure 15. Sequence of images of a simulation in which the vehicle overtakes a pedestrian with a steering maneuver.

Many situations have been simulated, with random initial positions and velocities of the vehicle and the pedestrian. In some cases the vehicle completely stops, without or with a small steering action. At other times, it decelerates and changes its direction, avoiding the pedestrian without come to a halt. In occasions, the vehicle slows down without completely stopping and without changing its direction, allowing pedestrians safely cross the region of interest. In a few cases, the car hits the pedestrian, but at very low speed.

V. Conclusions and Future Work

The mathematical model of an urban electric vehicle has been described and used for the development of a control strategy for the pedestrian avoidance maneuver in city traffic. At low level, a PI controller for throttle / brake and a P controller for the steering system are responsible for providing the necessary signals to the actuators. At a high level, simple kinematic formulas are used to determine the deceleration and direction necessary to prevent the accident.

It has been found that when the braking is not enough, it can be combined with a change in trajectory to avoid the pedestrian. But an abrupt change in the path may cause the vehicle to go out of its lane, causing an accident with more serious consequences with other vehicles or pedestrians. It is therefore desirable a system capable to detect this type of situation and decide if a steering maneuver is appropriate or not.

The experimental validation is still pending. This requires in first place completing the installation of sensors and actuators in the experimental vehicle. Secondly, it is intended to perform a battery of tests that allows a fine adjustment of the model, based on the data obtained from the sensors. Finally, other control strategies will be analyzed taking into account more complete information on the status of the vehicle and the environment.

Acknowledgment

This work is funded by the Spanish Ministry of Economy and Competitiveness, projects “Automatización y Control Inteligente de Vehículos Eléctricos Urbanos” (ACIVEU, DPI2012-36959) and “Assisted Navigation through Natural Language” (NAVEGASE, DPI2014-53525-C3-1-R).

References

[1] Dirección General de Tráfico, “Anuario estadístico de accidentes 2013”, Madrid, Spain. Ministerio del Interior, 2013.

[2] Wikipedia, “Collision avoidance system”, https://en.wikipedia.org/wiki/Collision_avoidance_system, Accessed May 24, 2015.

[3] Toyota, “Pedestrian-avoidance steer assist system”, http://www.toyota.com.cy/world-of-toyota/safety-technology/toyota-pedestrian-avoidance-steer-assist-system.json. Accessed August 15, 2015.

[4] D. Fernández Llorca, V. Milanés, I. Parra Alonso, M. Gavilán, I. García Daza, J. Pérez, M. A. Sotelo, “Autonomous pedestrian collision avoidance using a fuzzy steering controller”. IEEE Transactions on Intelligent Transportation Systems, Institute of Electrical and Electronics Engineers (IEEE), 12(2), 390-401, DOI: 10.1109/TITS.2010.2091272.

[5] Tirthankar Bandyopadhyay, Chong Zhuang Jie, David Hsu, Marcelo H. Ang Jr., Daniela Rus, Emilio Frazzoli, “Intention-aware pedestrian avoidance”, In Jaydev P. Desai, Gregory Dudek, Oussama Khatib, Vijay Kumar, editors, “Experimental Robotics. The 13th International Symposium on Experimental Robotics”, Springer International Publishing, 2013.

[6] L.A. Rentería, J.P. Oria, ”Genetic optimization of fuzzy adaptive cruise control for urban traffic”, In F. Matía, G. N. Marichal, E. Jiménez, editors, “Fuzzy Modeling and Control: Theory and Applications”, Atlantis Press, 2014.

[7] M.I. Arenado, J.P. Oria, C. Torre-Ferrero, L.A. Rentería, “Monovision-based vehicle detection, distance and relative speed measurement in urban traffic”, Intelligent Transport Systems, IET, 8(8), 655-664. DOI: 10.1049/iet-its.2013.0098.

[8] V. Milanés, L.A. Rentería, J. Villagrá, J. Godoy, T. de Pedro, J.P. Oria, “Traffic jam driving with NMV avoidance”, Mechanical Systems and Signal Processing, 31, 332-344. DOI: 10.1016/j.ymssp.2012.04.008.

[9] L.A. Rentería, V. Milanés, C. Torre-Ferrero, J. Godoy, J.P. Oria, T. de Pedro, “Ultrasonic sensors in urban traffic driving-aid systems”, Sensors, 11(1), 661-673. DOI: 10.3390/s110100661.

[10] T.D. Gillespie, “Fundamentals of vehicle dynamics”,. Society of Automotive Engineers, 1992..

[11] R. Rajamani, “Vehicle dynamics and control”, Springer US, 2012.

[12] H.B. Pacejka, “Tyre and vehicle dynamics”, Butterworth-Heinemann, 2006.

[13] J.C. Butcher, “Numerical methods for ordinary differential equations”, John Wiley & Sons, Ltd. 2008.